

Original Article

An experimental study on use of 7T MRI for evaluation of myocardial infarction in SD rats transfected with pcDNA 3.1(+)/VEGF₁₂₁ plasmid

Yan Zhang^{1,2}, Ruiqing Tian³, Xiangchun Shen⁴, Yushu Chen⁵, Wei Chen⁵, Lu Gan¹, Guiquan Shen², Haiyue Ju¹, Li Yang¹, Fabao Gao⁵

¹Department of Radiology General Hospital of PLA, Beijing 100853, PR China; ²Department of Radiology, Affiliated Hospital of Guizhou Medical University, Guiyang, PR China; ³Department of Oncology, The First People's Hospital of Guiyang, PR China; ⁴The Key Laboratory of Optional Utilization of Natural Medical Resource, Guizhou Medical University, University Town, Gui'an New District, Guiyang, PR China; ⁵Molecular Imaging Laboratory, Department of Radiology, West China Hospital, Sichuan University, PR China

Received March 30, 2016; Accepted May 20, 2016; Epub August 15, 2016; Published August 30, 2016

Abstract: This study aims to build the myocardial infarction model in SD rats transfected with pcDNA 3.1(+)/VEGF₁₂₁ plasmid and study the effect of the transfection using 7T MRI. Twenty-four male SD rats were randomly divided into 2 groups, pcDNA 3.1(+)/VEGF₁₂₁ plasmid transfection group (with improved coronary perfusion delivery) and myocardial infarction model group. Cardiac cine magnetic resonance imaging (Cine-MRI), T2-mapping and late gadolinium enhancement (LGE) cardiac imaging were performed at 24 h, 48 h, 72 h and 7 d after myocardial infarction, respectively. The signal intensity, area at risk (AAR), myocardium infarction core (MIC) and salvageable myocardial zone (SMZ) were compared. The hearts were harvested for anatomic characterization, which was related to pathological examination (TTC staining, HE staining, Masson staining and immunohistochemical staining). The Cine-MRI results showed that pcDNA 3.1(+)/VEGF₁₂₁ plasmid transfection group had higher end-diastolic volume (EDV) with a reduction in MIC and SMZ, as compared with the myocardial infarction model group. MIC, SMZ and AAR of the plasmid transfection declined over time. At 7 d, the two groups did not differ significantly in AAR and T2 value. According to Western Blotting, VEGF was up-regulated, while CaSR and caspase-3 were downregulated in the plasmid transfection group, as compared with the model group. In conclusion, a good treatment effect was achieved by coronary perfusion of pcDNA 3.1(+)/VEGF₁₂₁ plasmid. 7T CMR sequences provide a non-invasive quantification of the treatment efficacy. However, the assessment of myocardial injury using T2 value and AAR in the presence of edema is less accurate. The myocardial protection of the plasmid transfection group may be related to the inhibition of myocardial apoptosis, vascular endothelial cell (VEC) proliferation and collagen proliferation. The CaSR signaling pathway may contribute to reversing the apoptosis.

Keywords: Gene therapy, myocardial infarction, salvageable myocardial zone, myocardial infarction, CaSR

Introduction

Coronary artery occlusion can cause severe ischemic necrosis of the myocardia served by the infarcted artery. If the blood supply is not timely restored, myocardial infarction will spread from subendocardium to subepicardium. As a result, area at risk (AAR) (hibernating myocardium or stunned myocardium) will evolve into unsalvageable infarcted tissue, leading to abnormal cardiac function and heart failure. Although the application of coronary angioplasty or coronary artery bypass has alleviated cardiovascular diseases and prolonged patients' life, the mortality of myocardial infar-

tion remains high. Therefore, finding an appropriate technique of myocardial injury assessment and prognostic prediction is urgent for those with cardiovascular diseases.

We have found through preliminary experiment that pcDNA 3.1(+)/VEGF₁₂₁ plasmid transfection can reverse myocardial cell apoptosis and inhibit fibroblast proliferation. Transfection efficiency and the functions of secretory proteins were analyzed and the mechanism of myocardial cell apoptosis was discussed. For animal models, two issues are at stake: one is to choose the proper intervention pathway, and the other is how to evaluate the intervention

Evaluation of 7T MRI on myocardial infarction

effect. Gene therapy in rats can be implemented by coronary perfusion, intramyocardial injection or intrapericardial perfusion [1-3]. Following intramuscular injection of VEGF plasmid into the heart of pigs with chronic myocardial ischemia, the number of collateral vessels in the infarcted zone increased, with a great improvement of myocardial blood supply. Though this technique is effective, the myocardial injury will be too great for myocardial function evaluation. After literature review and preliminary experiments, we chose the coronary perfusion delivery technique, which not only achieves high transfection efficiency, but also reduces myocardial injury. In this study, 7T MRI was combined with several other imaging techniques for quantitative evaluation of the myocardial injury after 3.1(+)/VEGF₁₂₁ plasmid transfection in SD rats. The histological changes of the myocardium and the intensity changes of CMR sequences were characterized so as to evaluate the degree of myocardial ischemia and activity.

Materials and method

Grouping

Twenty-four healthy male SD rats were randomly divided into 2 groups (n=12), myocardial infarction model group and pcDNA 3.1(+)/VEGF₁₂₁ plasmid transfection group.

Construction of myocardial infarction model

Left anterior descending artery ligation was performed to induce myocardial infarction. For the plasmid transfection group, the heart and the ascending aorta were exposed and 20 μ l of the plasmid was injected into the ventricle. In the meantime, the circulation was blocked at the root of the ascending aorta for 5 s. The above procedures were repeated twice. Finally the thoracic cavity was closed and the rats were reared routinely.

MRI examination

Before imaging, anesthesia was induced using an anesthesia induction box (2.5% isoflurane, oxygen flow rate 1 L/min). Two to three minutes later, the rats were immobilized to the scanning bed in prone position. ECG leads were stuck to the four limbs, and a pad was placed under the abdomen to observe heart rate and respiratory rate. MRI was started after the heart rate and respiratory rate stabilized.

7T MRI evaluation of myocardial infarction in SD rats

CMR imaging was performed at 24 h, 48 h, 72 h and 7 d after modeling, respectively, in combination with FISP-Cine, T2 mapping and LGE imaging. Cine-MRI is mainly used for evaluating EDV of the left ventricle. The endocardium contour was traced manually in each slice at end diastole and end systole, and the thickness of each slice is added up together to obtain EDV. On the left ventricle images extracted at end diastole and end systole, ROI was delineated manually by each person for three times, and the average was taken (the measurements had good consistency. The interclass consistency coefficient (ICC) was calculated using SPSS 19.0 software, and the value was 1 for each sequence). The ventricle area including the myocardium and the chamber area excluding the myocardium were measured at end diastole and end systole for each sequence, respectively. On this basis, the increased thickness of myocardium of the left ventricle in this slice was calculated as the myocardial area at end systole minus the myocardial area at end diastole (myocardial area was equivalent to ventricle area minus the chamber area). Infarct region was defined as the myocardium where the signal intensity in LGE was larger than that of distant myocardium by a threshold of 5SD. SMZ was defined as the myocardium where the signal intensity was larger than that of distant myocardium by a threshold of 2SD on T2 maps. Cine-MRI images of the left ventricle at end systole were extracted, and ROIs of equal area were delineated in the myocardium. The signal intensity was measured for each ROI, and the mean and standard deviation of signal intensity of 6-8 ROIs in the left ventricle were calculated in each rat. The coefficient of variation was obtained. On this basis, AAR and MIC were delineated manually, and the difference between the two was SMZ. The infarct area on the CMR images was analyzed with Image J software, and for T2 mapping, special post-processing software was used. That is, the heart images were imported into the software, and the end-systolic and end-diastolic contours were delineated manually. The evaluation indicators of cardiac function were calculated.

Histological examination

Anatomic observation: The heart was harvested, photographed in the anatomical position

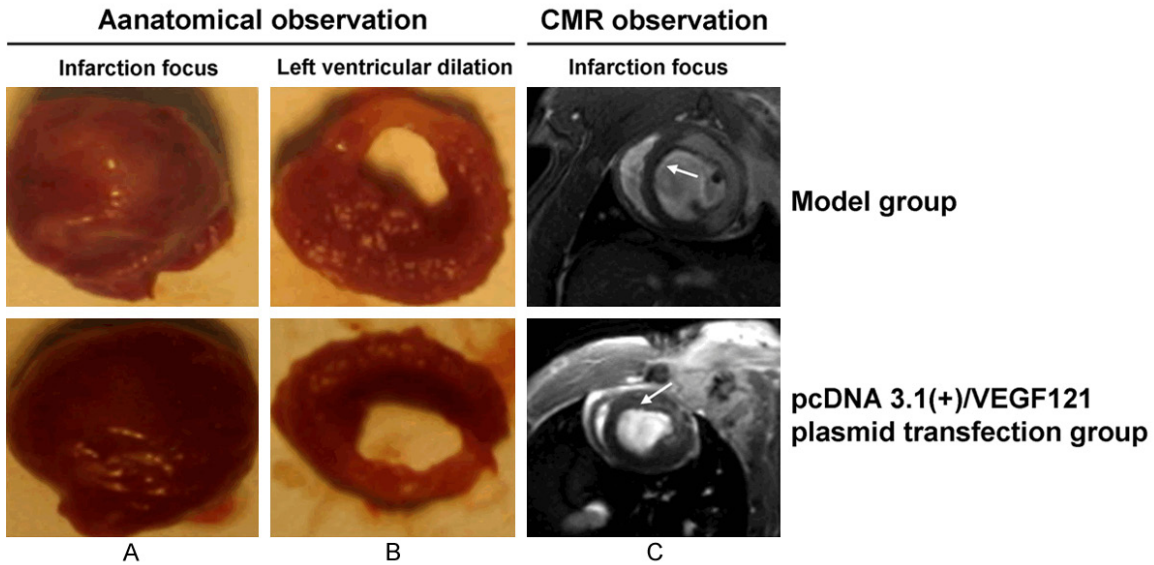


Figure 1. Anatomical and Cine-MRI observation for the heart of the model group and intervention group. A. Infarcts focus of the anatomical observation. B. Left ventricular dilation observation. C. Infarcts focus of the Cine-MRI observation. The white arrows illustrate the myocardial infarcts under the observation of the Cine-MRI.

and marked. The left ventricle was dissociated, the transverse section of the heart was harvested, photographed and marked.

TTC staining: After CMR imaging observation, the rats were sacrificed by intravenous injection of 10% potassium chloride, which arrested the heart in diastolic phase. The hearts were harvested for Masson staining and immunohistochemical staining.

Masson staining: Heart paraffin sections were subjected to Masson staining. Weigert's iron hematoxylin solution was added, followed by 1% hydrochloric acid in alcohol for differentiation. Then the sections were counterstained in xylidine-ponceau 2R, and sealed with neutral balsam. Under the low-power microscope, the collagen fibers and nuclei were stained blue, and the cytoplasm, muscle fibers and red blood cells were stained red. Photographs were taken and analyzed by the image analysis system.

Western blot detection of VEGF, CaSR and caspase-3

Total protein was extracted and identified. Tissues were taken out from liquid nitrogen and cut into pieces. Into every 100 mg of the tissue, 1 ml of TRIzol reagent was added. The tissues were made into homogenate on ice and incubated with lysis buffer at 15-30°C for 5 min. After centrifugation at 4°C at 12000×g for 10

min, the insolubles were removed. The solution was left to stand at room temperature for 5 min for full dissociation between the nucleic acids and the proteins. The standard curve was plotted, and the absorbance was measured at A590 nm. The protein concentration of the experimental group was calculated as follows: protein concentration of the experimental group=OD value of the experimental group × protein concentration of the standard well/OD value of the standard well). The average value was taken as the final result. SDS-PAGE was performed using 8-12% separating gel and 5% stacking gel. For each channel, 20 µl of the sample was loaded along with 20 µl of the marker. After electrophoresis, staining was performed with Coomassie Brilliant Blue R-250, followed by the addition of destaining solution. PVDF membrane of gel size was soaked in methanol for 15 s, washed with dH₂O and balanced with transfer buffer for 5 min. The proteins were blotted to the PVDF membranes by semi-dry electrotransfer. Then the membranes were placed into a plastic bag and sealed with blocking buffer for 2 h. The membranes were washed with TBST for 3 times for 10 min each time, then incubated with primary antibodies at 4°C overnight or at room temperature for 2 h. The membranes were washed again with TBST for 3 times for 10 min each time, then with TBS for 10 min. Immune complexes were detected using ECL Western Blot Detection Kit.

Evaluation of 7T MRI on myocardial infarction

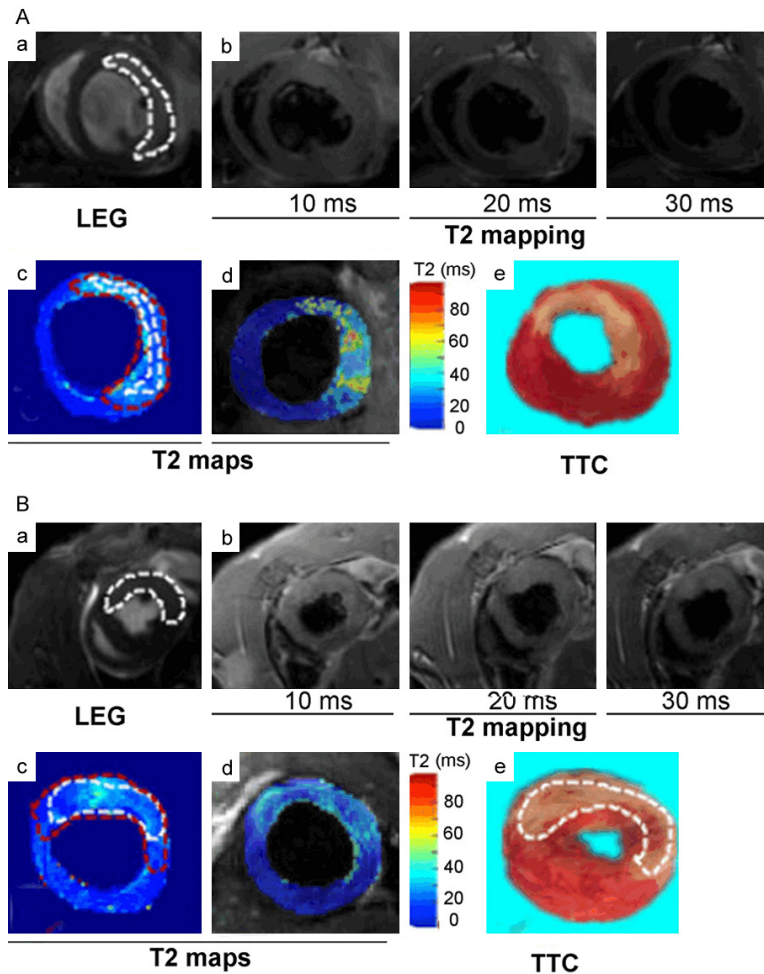


Figure 2. Observation for the infarct areas and AAR at 24 h in MRI and TTC staining. A. Infarct areas in pcDNA3.1(+)/VEGF₁₂₁ transfection group. a. LGE image; b. T2 mapping scanned by MRI; c and d. Pseudo-color maps infarct areas; d. TCC staining; e. This image was made by 2,3,5-triphenylterazolium chloride staining (TTC) in two groups, the difference between infarction size and the viable myocardium was stained red or white. B. Infarct areas in model group. a. LGE image; b. T2 mapping scanned by MRI; c and d. Pseudo-color maps infarct areas; d. TCC staining; e. This image was made by 2,3,5-triphenylterazolium chloride staining (TTC) in two groups, the difference between infarction size and the viable myocardium was stained red or white.

The membranes were exposed and scanned using SK-100 Image System. The grayscale ratio of the target band to the β -action band was calculated as the relative expression of the target gene. Four replicates were done for Western Blot.

Statistical analysis

The measurements were expressed as Mean \pm SD. Paired t-test was used for pairwise comparison, and independent-samples t-test was used to compare T2 values of different myocardial segments in the same group. For mul-

tipole group comparison of T2 values, one-way ANOVA was carried out, with testing for normality and homoscedasticity. $P < 0.05$ indicated significant differences. All statistical analyses were carried out using SPSS 19.0 software.

Results

Survival of rats and anatomical observation of hearts at 24 h

Excluding the rats which died during surgery and scanning due to ventricular fibrillation and those with poor image quality, 20 rats were finally included (10 in the model group and 10 in the plasmid transfection group). Infarct region was observed in both two groups by CMR at 24 h after modeling. Cine-MRI indicated that average EDV was $84.3 \pm 6.34 \mu\text{l}$ vs. $98.8 \pm 7.24 \mu\text{l}$ for the two groups ($P < 0.01$, $n = 16$).

By anatomical observation, it can be seen that the plasmid transfection group had less severe infarction and the infarcts were transparent and grayish white (Figure 1A), as compared with the model group. Left ventricular dilation can be observed in the figure below (Figure 1B). By CMR

observation, the results indicated that the plasmid transfection group significantly improved the infarction compared to the model group (Figure 1C).

Comparison of infarct areas and AAR at 24 h in MRI and TTC staining

LGE imaging indicated white myocardium in the two groups (Figure 2Aa, 2Ba), which correspondences to the “bright regions” in MRI. T2 mapping also showed the infarct areas (Figure 2Ab, 2Bb), which were hyperintense compared

Evaluation of 7T MRI on myocardial infarction

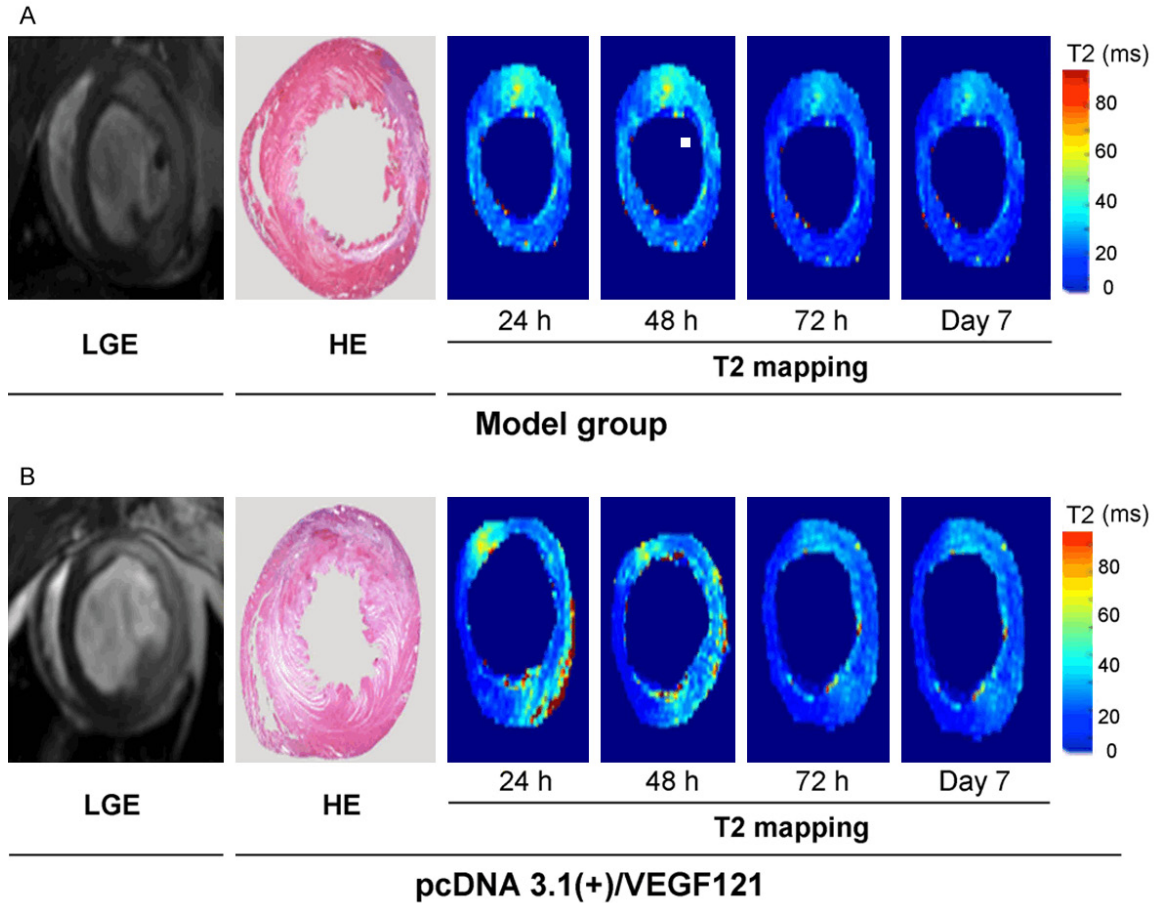


Figure 3. Observation for the MIC by using the LGE imaging, HE staining and T2 mapping. A. Model group. B. pcDNA3.1(+)/VEGF₁₂₁ group.

with other regions. Pseudo-color maps were generated with Image J and special post-processing software for T2 mapping. ROIs of myocardial infarction were delineated manually, from which AAR was obtained (Figure 2Ac, 2Ad, 2Bc, 2Bd). The distributions of infarct areas and AAR were basically consistent in LGE imaging and TTC staining (Figure 2Ae, 2Be). Meanwhile, the results indicated that the infarct areas in pcDNA 3.1(+)/VEGF₁₂₁ transfection group was significantly decreased compared to the control group (Figure 2).

Comparison of LGE imaging of MIC against HE staining

LGE imaging results were consistent with HE staining at 24 h (Figures 3, 4A, 4B). MIC was measured at different time points from 24 h to 7 d by LGE imaging. According to his tological staining, MIC was significantly small er in the

intervention group as compared with the model group. Such difference was most prominent at 7 d, with the result of $32.8 \pm 2.91 \mu\text{l}$ vs. $27.4 \pm 1.90 \mu\text{l}$ ($P < 0.01$, $n = 6$). LGE imaging results of MIC agreed well with that of HE staining; MIC of both two groups declined over time (Figures 3, 4A, 4B).

Changes of AAR and T2 value by T2 mapping over time

AAR was evaluated by T2 mapping for the two groups from 24 h to 7 d. It was found that AAR of the intervention group was significantly smaller than that of the model group, but the two groups had similar AAR at 7 d (Figures 3, 4C). Within 72 h after modeling, T2 value declined gradually, and the two differed significantly in T2 value, especially at 72 h (Figures 3, 4D). At 7 d, T2 values increased in both two groups, without significant difference (Figures 3, 4).

Evaluation of 7T MRI on myocardial infarction

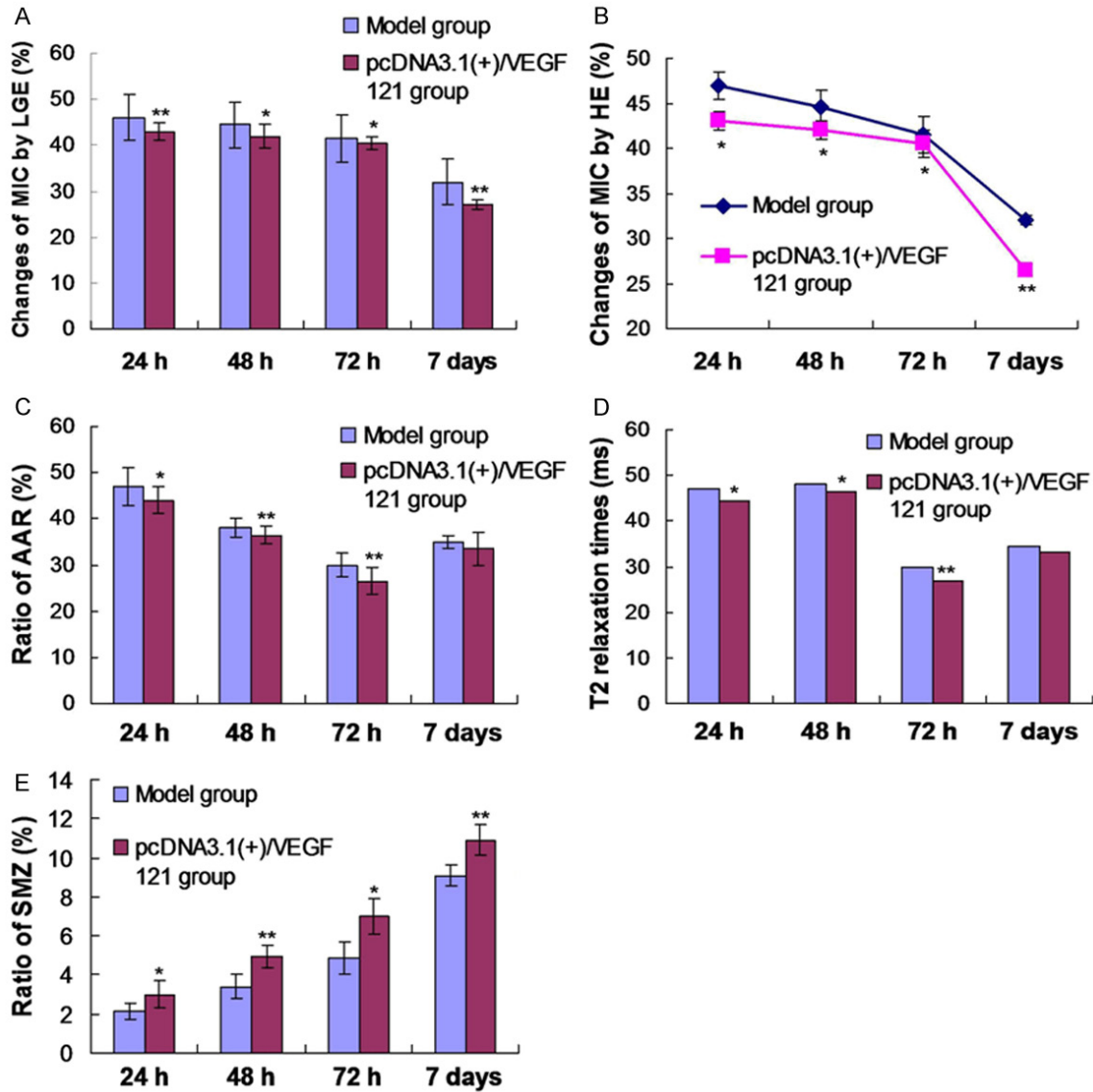


Figure 4. Changes of MIC ratio, AAR, T2 relaxation times and SMZ ratio in myocardium by T2 mapping. A. Ratio changes of MIC by LGE in both model group and pcDNA 3.1(+)/VEGF₁₂₁ group ($\bar{x} \pm s$, 24 h, n=10; 48 h-7 d, n=6). B. Ratio changes of MIC by HE in both model and pcDNA 3.1(+)/VEGF₁₂₁ group. C. Apparent AAR changes in myocardium by T2-mapping. The T2 mapping shows the edema area as AAR after ischemic infarction in both model group and pcDNA 3.1(+)/VEGF₁₂₁ group. All T2 maps were scaled between 0 and 80 ms. ($\bar{x} \pm s$, 24 h n=10; 48 h-7 d, n=6). D. Apparent T2 relaxation times in myocardium by T2 mapping. T2 mapping shows T2 relaxation times after ischemic infarction in both model and pcDNA 3.1(+)/VEGF₁₂₁ groups. ($\bar{x} \pm s$, 24 h, n=10; 48 h-7 d, n=6). E. Apparent SMZ is equal to AAR minus MIC. The graph indicates SMZ after ischemic infarction in both model group and pcDNA 3.1(+)/VEGF₁₂₁ group ($\bar{x} \pm s$, 24 h, n=10; 48 h-7 d, n=6). *p<0.05, **p<0.01 vs model group.

Comparison of SMZ

SMZ was equivalent to AAR minus MIC. From 24 h to 72 h, SMZ declined gradually in both two groups, and the intervention group had much smaller SMZ than the model group. At 7 d, SMZ increased significantly in the model group, as shown in **Figure 4E**.

Histological staining

Masson staining, HE staining and immunohistochemical staining for CD31 revealed infarct areas in both two groups. Some myocardial cells shrank, with disordered arrangement and spot-like bleeding in the ruptured myocardium. The myocardial injury was more severe in the

Evaluation of 7T MRI on myocardial infarction

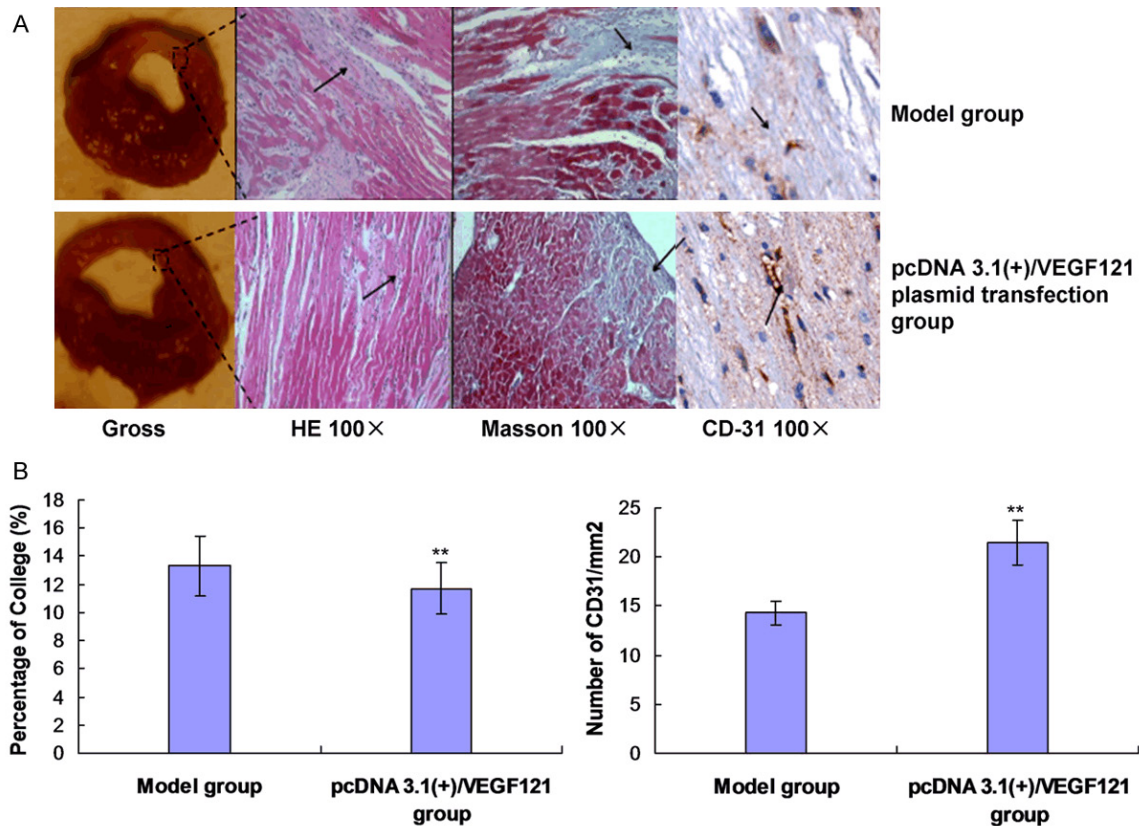


Figure 5. Evaluation for the myocardium infarction in gross tissue after 7 days in model group and pcDNA 3.1(+)/VEGF₁₂₁ group. A. Histological sections stained with hematoxylin and eosin show features of myocardium changes after 7 day. collagen was stained blue. The CD31 was stained by using the immunohistochemical analysis. B. Statistical analysis for the collagen and CD-31 staining. The sections were stained with anti-collagen and anti-CD31, respectively. All data are expressed as mean SEM, and the difference were illustrated between the two groups.

model group, where extensive necrosis of myocardial cells was found, nuclei disappeared and vacuoles were formed; the necrotic region was featured by severe hyperplasia of connective tissues. Masson staining indicated myocardial fiber hyperplasia. By immunohistochemical staining, more cells were stained in the intervention group than in the model group, indicating endothelial cell proliferation (**Figure 5A, 5B**).

Western blot detection of VEGF, CaSR and caspase-3

Western Blot showed that VEGF was significantly up-regulated after the transfection, as compared with the model group ($P < 0.05$, **Figure 6A**). CaSR ($P < 0.05$, **Figure 6B**) and caspase-3 ($P < 0.05$, **Figure 6C**) were down-regulated significantly in the intervention group.

Discussion

Several therapies are now in use for treating ischemic heart disease, including percutaneous coronary angioplasty, stent implantation, coronary artery bypass and medication treatment. These therapies can alleviate the symptoms of cardiac insufficiency, but the methods for efficacy evaluation are generally traumatic. Moreover, the patients are still faced with the risk of heart failure [4]. Myocardial cell apoptosis and fibroblast proliferation during myocardial infarction are important pathology of heart failure. Instead of focusing on the therapeutic angiogenesis of VECs, we found that pcDNA 3.1(+)/VEGF₁₂₁ plasmid transfection reversed myocardial cell apoptosis and inhibited fibroblast proliferation. Stem cells are now increasingly applied to cellular therapy [5], but there may still be the probability that stem cells do

Evaluation of 7T MRI on myocardial infarction

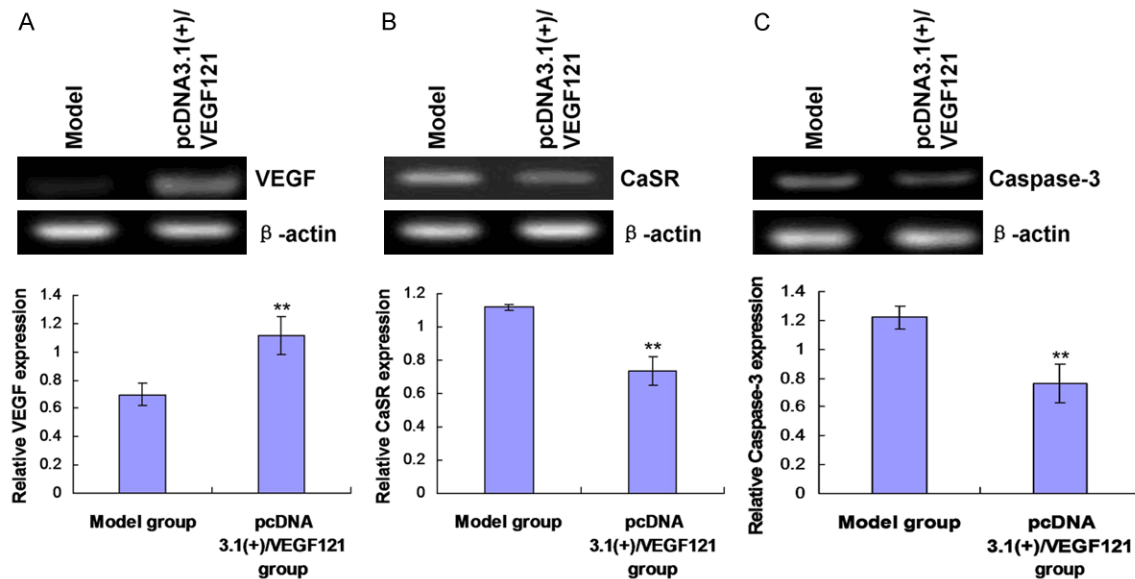


Figure 6. Relative expression of the VEGF, CaSR and Caspase-3 in model group and pcDNA 3.1(+)/VEGF₁₂₁ group ($\bar{x} \pm s$, n=4). VEGF, CaSR and Caspase-3 levels were analyzed by Western Blot using the anti-VEGF/CaSR/Caspase-3 antibody. A. Examination and statistical analysis for VEGF expression. B. Examination and statistical analysis for CaSR expression. C. Examination and statistical analysis for Caspase-3 expression. The immunoblots shown were obtained from 4 independent experiments. Levels of VEGF/CaSR/Caspase-3 were shown as a percentage of change in the mean value derived from 4 independent experiments ($\bar{x} \pm s$, n=4). *p<0.05, **p<0.01 vs model group.

not differentiate into myocardial cells, but into other types of cells, leading to severe calcification [6]. Many studies have been carried out on the use of VEGF in treating coronary heart disease. In vitro experiment has found that VEGF is involved in coronary artery circulation, inducing the upregulation of VEGF protein and mRNA, promoting angiogenesis and anti-apoptotic effect [7]. As proved by a large amount of experiments, VEGF promotes the formation of capillary network and hence collateral circulation in ischemic myocardium [8-10]. But the anti-apoptotic role of VEGF in the myocardium is less mentioned. Considering the high cost and the need for repeated VEGF injection, the adenoviral vector carrying VEGF is injected. However, the short length of action has restricted its application. Another method is myocardial transfection of high-purity plasmid.

The genes can be delivered by coronary perfusion, intramyocardial injection and intrapericardial injection. One study [11] performed intramuscular injection of VEGF-carrying plasmid into the heart of pigs with chronic myocardial ischemia and found that the number of collateral vessels increased in the infarct region. This indicated good treatment effect of VEGF in

ischemic myocardium, but this method can cause great myocardial injury. In this experiment, coronary perfusion delivery technique was chosen, with the blocking of blood flow at the root of ascending aorta for 5 s. This would stop the systolic blood flow of the ventricle in systemic circulation, with an increase in diastolic intracoronary pressure and transfection efficiency. In contrast, transfection by intravenous injection usually has a low efficiency, intramyocardial injection causes too great damage, and intrapericardial injection has uncertain effect. By using coronary perfusion, the transfection efficiency is greatly improved. Moreover, with the blocking of blood flow at the root of ascending aorta twice for 5 s each time, the contact between the plasmid and the heart wall is increased, thus reducing the perfusion injury.

We have demonstrated the treatment effect of transfection of VEGF-carrying plasmid in myocardial infarction through preliminary experiment. In this paper, SD rat model of myocardial infarction was built, and the myocardial injury induced was evaluated by CMR. At 24 h after modeling, infarct regions were revealed in both groups. EDV of the two groups was 84.3 ± 6.34

Evaluation of 7T MRI on myocardial infarction

μl vs. $98.8 \pm 7.24 \mu\text{l}$ ($P < 0.01$, $n = 10$). According to anatomical observation, the left ventricle contained infarct regions in the intervention group, which were transparent and grayish white but were less severe than in the model group. AAR and MIC were measured by LGE from 24 h to 7 d. MIC of the intervention group was significantly smaller than that of the model group, especially at 7 d, which was $32.8 \pm 2.91 \mu\text{l}$ vs. $27.4 \pm 1.90 \mu\text{l}$ ($P < 0.01$, $n = 6$). LGE imaging results agreed well with HE staining for the detection of MCI; both groups showed a decrease of MCI over time. By T2 mapping, AAR of the intervention group decreased from 24 h to 72 h and was significantly lower than that of the model group. AAR started to increase at 7 d, and the two groups showed no significant difference. Within the first 72 h, T2 values decreased over time in the two groups; the two groups were significantly different, and the difference was the greatest at 72 h. T2 value began to increase at 7 d in the two groups. This result suggested the protective effect of pcDNA 3.1(+)/VEGF₁₂₁ plasmid in ischemic myocardium, but the working mechanism is still uncertain.

After the first research [16] on the relationship between T2 mapping and edema, G et al. [17] later identified 2 peaks of T2 value at 1-7 d after myocardial infarction in swine model. This phenomenon has been observed by many other researchers [18, 19]. By measuring the water content of the infarct area, the first peak can be attributed to reperfusion injury or stress-induced edema following myocardial infarction. The second peak is not related to edema, but to collagen hyperplasia during the healing of the ischemic myocardium. This hypothesis was then proved by comparing with pathological results. Similar conclusions were obtained in this study, which proved the value of T2 mapping in differentiating reversible myocardial injury and diagnosing acute myocardial infarction. Increased T2 value after edema should be interpreted with caution. At 7 d after modeling, there was an increase in AAR and T2 value, which may be related to spontaneous healing of the ischemic myocardium. To verify this, Masson staining and immunochemical staining for CD31 were performed. HE staining indicated infarct regions in both groups, with model group having more severe myocardial fiber hyperplasia. By immunohistochemical staining,

more cells were stained positively in the intervention group than in the model group. It was therefore confirmed that collagen hyperplasia was more effectively inhibited and VEC proliferation was promoted in the intervention group.

We further evaluated the treatment effect of pcDNA 3.1(+)/VEGF₁₂₁ plasmid transfection in rat model by Western Blot. The result showed that VEGF was significantly upregulated in the intervention group than in the control group. CaSR is involved in maintaining the homeostasis of Ca^{2+} and other metal ions, regulating myocardial cell differentiation, apoptosis and necrosis. Our preliminary study has shown that VEGF can reverse myocardial cell apoptosis by inhibiting CaSR expression. By building the animal model of myocardial infarction, we found that CaSR was greatly upregulated, while pcDNA 3.1(+)/VEGF₁₂₁ plasmid transfection caused an obvious reduction in CaSR expression. This indicated similar treatment effect as in the cellular model and agreed with the findings by other researchers [25, 26]. Caspase-3 is activated in the apoptotic cells both by extrinsic (death ligand) and intrinsic (mitochondrial) pathways [27, 28]. Caspase family members act as the executors of apoptosis. In normal conditions, caspases exist in the cytoplasm in the form of proenzymes. Once activated by external stimuli, caspase 3 can degrade specific substrates, leading to DNA fracture, chromatin condensation and formation of apoptotic bodies. It was found by Western Blot that pcDNA 3.1(+)/VEGF₁₂₁ plasmid transfection greatly downregulated caspase-3. Moreover, SMZ and AAR measured by CMR can be used as indicators of the treatment effect of pcDNA 3.1(+)/VEGF₁₂₁ plasmid transfection in rat model of myocardial infarction.

pcDNA 3.1(+)/VEGF₁₂₁ plasmid transfection effectively reduced MIC, as compared with the myocardial infarction model group and VEGF-carrying plasmid transfection group. SMZ can be used as a reliable indicator of the treatment effect. T2 value and AAR measured by T2 mapping have high value in evaluating myocardial infarction at the acute stage, but they may be less accurate if edema happens. Increased T2 value may not indicate the second peak of edema, but the spontaneous healing of the ischemic myocardium. VEGF-carrying plasmid transfection can help increase SMZ, and inhibit

Evaluation of 7T MRI on myocardial infarction

myocardial cell apoptosis, VEC proliferation and collagen hyperplasia.

Acknowledgements

This study was granted by the Health and Family Planning Commission of GuiZhou Province (Grant No. WT-201405) and postdoctoral Sustentation Fund of PLA (NO. 20100471818).

Disclosure of conflict of interest

None.

Address correspondence to: Dr. Li Yang, Department of Radiology General Hospital of PLA, No. 28 Fuxing Road 100853, Beijing, PR China. Tel: +86-010-66939564; E-mail: yangli301@yahoo.com; Dr. Fabao Gao, Molecular Imaging Laboratory, Department of Radiology, West China Hospital, Sichuan University, No. 37 Guoxuexiang 610041, Chengdu, PR China. E-mail: gaofabao@yahoo.com

References

- [1] Hosoyama T, Samura M, Kudo T, Nishimoto A, Ueno K, Murata T, Ohama T, Sato K, Milkamo A, Yoshimura K, Li TS, Hamano K. Cardiosphere-derived cell sheet primed with hypoxia improves left ventricular function of chronically infarcted heart. *Am J Transl Res* 2015; 7: 2738-2751.
- [2] Du GQ, Du WJ, Liu JJ, Wang YS, Nie HG, Zhang MM, Yu B. Wnt1-overexpressing skeletal myoblasts as an improved cell therapy for cardiac repair following myocardial infarction. *Panminerva Med* 2015; 57: 153-166.
- [3] Yla-Herttuala S, Martin F. J cardiovascular gene therapy. *Lancet* 2000; 355: 213-222.
- [4] Skouri HN, Dec GW, Friedrich MG, Cooper LT. Noninvasive imaging in myocarditis. *J Am Coll Cardiol* 2006; 2085-2095.
- [5] Vandergriff AC, HensleyTM, Henry ET, Shen D, Anthony S, Zhang J, Cheng K. Magnetic targeting of cardiosphere-derived stem cells with ferumoxytol nanoparticles for treating rats with myocardial infarction. *Biomaterials* 2014; 35: 8528-8539.
- [6] Ong P, Athansiadis A, Hill S, Kispert EM, Borgulya G, Klingel K, Kandolf R, Sechtem U, Mahrhoth H. Usefulness of Pericardial Effusion as New Diagnostic Criterion for Noninvasive Detection of Myocarditis. *Am J Cardiol* 2011; 108: 445-452.
- [7] Friedrich MG, Sechtem U, Schulz-Menger J, Holmvang G, Alakija P, Cooper LT, White JA. International Consensus Group on Cardiovascular Magnetic Resonance in Myocarditis, Cardiovascular magnetic resonance in myocarditis: A JACC White Paper. *J Am Coll Cardiol* 2009; 53: 1475-1487.
- [8] Madonna R, Petrov L, Teberino MA. Transplantation of adipose tissue mesenchymal cells conjugated with VEGF-releasing microcarriers promotes repair in murine myocardial infarction. *Cardiovasc Res* 2015; 108: 39-49.
- [9] Lee S, Chen TT, Barber CL, Jordan MC, Murdock J, Desai S, Ferrara N, Nagy A, Roos KP, Iruela-Arispe ML. Autocrine VEGF signaling is required for vascular homeostasis. *Cell* 2007; 130: 691-703.
- [10] Yang Y, Shi C, Hou X. Modified VEGF targets the ischemic myocardium and promotes functional recovery after myocardial infarction. *J Control Release* 2015; 213: 27-35.
- [11] Liu R, Guo C, Yang C, Xu D, Wang C. VEGF165 attenuates the Th17/Treg imbalance that exists when transplanting allogeneic skeletal myoblasts to treat acute myocardial infarction. *Inflamm Res* 2013; 62: 69-79.
- [12] Miao WF, Luo Z, Kises RN, Walsh K. Intracoronary adenovirus-mediated Akt gene transfer in heart limits infarct size following ischemia-reperfusion injury in vivo. *J Mol Cell Cardiol* 2000; 32: 2397-2402.
- [13] Hausenloy DJ, Yellon DM. Time to take myocardial reperfusion injury seriously. *N Engl J Med* 2008; 359: 518-520.
- [14] Kim RJ, Chen EL, Lima JA, Judd RM. Myocardial Gd-DTPA kinetics determine MRI contrast enhancement and reflect the extent and severity of myocardial injury after acute reperfused infarction. *Circulation* 1996; 94: 3318-3326.
- [15] Naßenstein K, Nensa F, Schlosser T, Bruder O, Umütlu L, Lauenstein T, Maderwald S, Ladd ME. Cardiac MRI: T2-Mapping Versus T2-Weighted Dark-Blood TSE Imaging for Myocardial Edema Visualization in Acute Myocardial Infarction. *Rofo* 2014; 186: 166-172.
- [16] Higgins CB, Herfkens R, Lipton MJ, Sievers R, Sheldon P, Kaufman L, Crooks LE. Nuclear magnetic resonance imaging of acute myocardial infarction in dogs: alterations in magnetic relaxation times. *Am J Cardiol* 1983; 52: 184-188.
- [17] Fernández-Jiménez R, García-Prieto J, Sánchez-González J. Pathophysiology Underlying the Bimodal Edema Phenomenon After Myocardial Ischemia/Reperfusion. *J Am Coll Cardiol* 2015; 66: 816-828.
- [18] Zia MI, Ghugre NR, Connelly KA, Strauss BH, Sparkes JD, Dick AJ, Wright GA. Characterizing myocardial edema and hemorrhage using quantitative T2 and T2* mapping at multiple time intervals post ST-segment elevation myocardial infarction. *Circ Cardiovasc Imaging* 2012; 5: 566-572.

Evaluation of 7T MRI on myocardial infarction

- [19] Zech WD, Schwendener N, Persson A, Warn-tjes MJ, Jackowski C. Postmortem MR quantification of the heart for characterization and differentiation of ischaemic myocardial lesions. *Eur Radiol* 2015; 25: 2067-2073.
- [20] Treible TA, White SK, Moon JC. Myocardial tissue characterization: histological and pathophysiological correlation. *J Curr cardiovasc Imaging Rep* 2014; 7: 9254-9259.
- [21] Klonet RA, Fishbein MC, Lew H, Maroko PR, Braunwald E. Mummification of the infarcted myocardium by high dose corticosteroids. *Circulation* 1978; 57: 56-63.
- [22] Bönner F, Janzarik N, Jacoby C. Myocardial T2 mapping reveals age- and sex-related differences in volunteers. *J Cardiovasc Magn Reson* 2015; 17: 15-18.
- [23] Langhans B, Nadjiri J, Jähnichen C. Reproducibility of area at risk assessment in acute myocardial infarction by T1- and T2-mapping sequences in cardiac magnetic resonance imaging in comparison to Tc99m-sestamibi SPECT. *Int J Cardiovasc Imaging* 2014; 30: 1357-1363.
- [24] Xia R, Lu X, Zhang B, Wang Y, Liao J, Zheng J, Gao F. Assessment of myocardial edema and area at risk in a rat model of myocardial infarction with a faster T2 mapping method. *Acta Radiol* 2015; 56: 1085-1090.
- [25] Sun YH, Liu MN, Li H, Shi S, Zhao YJ, Wang R, Xu CQ. Calcium-sensing receptor induces rat neonatal ventricular cardiomyocyte apoptosis. *Biochem Biophys Res Commun* 2006; 350: 942-948.
- [26] Feng SL, Sun MR, Li TT, Yin X, Xu CQ, Sun YH. Activation of calcium-sensing receptor increases TRPC3 expression in rat cardiomyocytes. *Biochem Biophys Res Commun* 2011; 406: 278-284.
- [27] Asa B, Gustafsson, Robert A. Gottlieb. Heart mitochondria: gates of life and death. *Cardiovas Res* 2008; 77: 334-343.
- [28] Tan WQ, Wang JX, Lin ZQ, Li YR, Lin Y, Li PF. Novel Cardiac Apoptosis Repressor With Caspase Recruitment Domain by Calcineurin. *Circulation* 2008; 118: 2268-2276.